

REPORT DOCUMENTATION PAGE

Public reporting burden for this collection of information is estimated to average 1 hour per response, including gathering and maintaining the data needed, and completing and reviewing the collection of information. Send collection of information, including suggestions for reducing this burden, to Washington Headquarters Service, Davis Highway, Suite 1204, Arlington, VA 22202-4302, and to the Office of Management and Budget, Paperwork Project, Washington, DC 20503.

AFRL-SR-AR-TR-03-

0257

Source,
of this
person

1. AGENCY USE ONLY (Leave blank)		2. REPORT DATE 09-JULY-2003	3. REPORT TYPE AND DATES COVERED FINAL (15-JAN-2001 TO 31-DEC-2001)
4. TITLE AND SUBTITLE CONTINUED COMPUTATIONAL INVESTIGATION OF MEMS - HYBRID SURFACES			5. FUNDING NUMBERS F49620-01-1-0169
6. AUTHOR(S) DAVID B. GOLDSTEIN			
7. PERFORMING ORGANIZATION NAME(S) AND ADDRESS(ES) CENTER FOR AEROMECHANICS RESEARCH DEPT. OF AEROSPACE ENGINEERING & ENGINEERING MECHANICS THE UNIVERSITY OF TEXAS AT AUSTIN AUSTIN, TX 78712-1085			8. PERFORMING ORGANIZATION REPORT NUMBER
9. SPONSORING/MONITORING AGENCY NAME(S) AND ADDRESS(ES) AFOSR/NA 4015 WILSON BOULEVARD ARLINGTON, VA 22203			10. SPONSORING/MONITORING AGENCY REPORT NUMBER
11. SUPPLEMENTARY NOTES			
12a. DISTRIBUTION AVAILABILITY STATEMENT Approved for public release; distribution unlimited.			12b. DISTRIBUTION CODE
13. ABSTRACT (Maximum 200 words) Flow control may be achieved by using MEMS to alter the fine scale flow structures within a boundary layer. We here report on a detailed direct numerical simulation of slot jet MEMS for the purpose of flow control. Individual pulses were aimed at specific boundary layer structures, or were created in a flow "combed" by riblets. A feedback control method is also studied and used to calibrate the strength of actuation to match flow conditions. This final report, on a one-year project funded between two longer term related projects, describes a few conclusive findings as well as work in progress.			
14. SUBJECT TERMS			15. NUMBER OF PAGES 6
			16. PRICE CODE
17. SECURITY CLASSIFICATION OF REPORT UNCLASSIFIED	18. SECURITY CLASSIFICATION OF THIS PAGE UNCLASSIFIED	19. SECURITY CLASSIFICATION OF ABSTRACT UNCLASSIFIED	20. LIMITATION OF ABSTRACT

BEST AVAILABLE COPY

20030731 083

Continued Computational Investigation of MEMS - Hybrid Surfaces**GRANT NUMBER F49620-01-1-0169****FINAL REPORT****David B. Goldstein**

Center for Aeromechanics Research

Department of Aerospace Engineering & Engineering Mechanics

The University of Texas at Austin

Austin, TX 78712-1085

Abstract

Flow control may be achieved by using MEMS to alter the fine scale flow structures within a boundary layer. We here report on a detailed direct numerical simulation of slot jet MEMS for the purpose of flow control. Individual pulses were aimed at specific boundary layer structures, or were created in a flow "combed" by riblets. A feedback control method is also studied and used to calibrate the strength of actuation to match flow conditions. This final report, on a one year project funded between two longer term related projects, describes a few conclusive findings as well as work in progress.

Background

A turbulent boundary layer is characterized by coherent vortical structures that arise, evolve and decay in a quasi-periodic fashion. Of particular interest are the streamwise vortices that lead to the formation of velocity streaks. Such streaks are believed to be responsible for key mechanisms in turbulence production and increased shear stress [1]. Consequently, substantial reductions in drag may be achieved by wall-mounted actuators operating on the streaks to either stabilize the flow or reduce shear [2]. Indeed, a continuous distribution of blowing and suction in direct numerical simulations of turbulent channel flows have been successful in reducing wall shear stress [3]. Experimentally, some flow control was obtained with a system containing multiple sensors and microjet MEMS actuators [4]. However, reported drag reductions, such as [5], were mostly due to reductions in pressure drag, as opposed to the manipulation of structures within the turbulent boundary layer. Thus, practical devices able to achieve fine flow control at the small scales near the surface remain to be developed and their detailed interaction with a boundary layer remains to be determined.

Our numerical studies [6,7] have shown that when continuously operated in a turbulent boundary layer, small MEMS devices can substantially affect structures well beyond the buffer layer but were not found to decrease drag on the surface. Thus, it still remains to be determined if and how reasonably realistic slot jets can be useful for active flow control. On the other hand, several forms of passive textures such as riblets aligned in the streamwise direction have reduced drag between 4 - 10% [8,9]. These results have been examined numerically in our group [10], where it was determined that riblets work by dampening the spanwise fluctuations of the flow near the surface. This finding suggested that riblets may also produce more coherent near-wall vortical structures making them more easily identifiable and perhaps controllable.

Objectives

The goals of this study are to expand upon the work in [6] and [7]. We examine the potential of several configurations for flow control. First, we examine the interaction of single pulses aimed at particular structures responsible for or indicative of high shear stress. Second, we examine the amount of "combing" provided by riblets as well as the interaction and evolution of a jet pulse adjacent to a riblet. Last, we systematically examine the feedback control algorithm used successfully in [3] and apply it to multiple, discrete actuators which can serve as a basic model for a practical device for flow

control.

DNS Method and Initial Simulation Domain

The spectral method is based on that in [11]. Please refer to references [6-7] and related publications for more details and issues related to validation and convergence.

The domain consists of a rectangular channel with mean flow in the x-direction. Flow is periodic in both the x and z directions while the horizontal y-planes are defined as the channel boundaries. The actuators are constructed by inserting a virtual surface containing slots above the bottom of the channel (fig. 1). In the space between the plate and the lower channel wall, dividing walls spanning the length of the domain are placed to create the jet cavities such that each actuator unit consists of two slot jets powered by a common membrane (fig. 1 inset). The membranes are rectangular sections of the divider wall in which the force field method imposes a time-varying velocity in the z-direction.

Effects of Single Pulse Actuation of Slot Jets

The effect of single actuator pulses on turbulent boundary layer structures was studied by selecting appropriate instances in which particular structures would pass over one of the slot jets. The simulation was then rewound and the devices set to blow a single pulse. Two types of single actuation were tested: a steered jet, tilted 45° from the normal direction and a strong jet, twice as strong but having the same impulse magnitude as the steered jet. In both cases, a blowing pulse was created and its subsequent interaction with the target structures was followed over several thousand time steps. Flow events and their evolution were compared to an un-actuated case spanning the same time interval.

In the case of the steered jet, a single blowing pulse was aimed ahead of a streamwise vorticity "worm" so that the resulting hairpin would interact with the target structure. For the strong jet, a blowing pulse from both center slots was aimed directly underneath a large enstrophy "pancake" structure in an attempt to displace it (fig. 2a). In both cases, the pulses were able to eliminate the original structures. However, the pulses also created more enstrophy "pancake" structures and as the jets rose, several rising tendrils of vorticity were left in their wake (fig. 2b). In the case of the strong jet, limiting actuation to a single blowing slot showed that the pulse blew through the large target structure and still produced the same result of rising tendrils of vorticity. Consequently, for all cases, comparison between the drag for the undisturbed flow and the actuated flow over a short period of time indicated marginal increases in drag due to actuation.

Hybrid Surfaces

The above single pulses were unable to provide useful flow control due to the tendency of the jets to introduce new vorticity or at least cause greater vertical mixing of the flow. Thus, it was thought that hybrid surfaces combining passive elements and active devices would be useful in re-orienting and re-organizing the turbulent structures prior to actuation.

To better isolate the effect of a single slot, the computational domain was modified to contain only 1 actuator with slots 3 times larger than previously used. The passive elements chosen were streamwise cusped riblets spanning the length of the channel. Initially, two riblets, placed $100l^*$ apart were able to contain the pancake boundary layer structures between them. Also, concentrated regions of high enstrophy very often slid along the crest of the riblets (fig. 3a). An additional riblet placed between the original pair (making the riblet spacing $50l^*$) completely lifted the pancake boundary layer structures away from the surface and onto the crests of the riblets. A single pulse out of one slot adjacent to a riblet (fig. 3b) produced a hairpin vortex shifted in the spanwise direction toward the riblet so that the legs of the hairpin straddled the riblet before dissipating. Despite this Coanda-like effect, pulses were unsuccessful in eliminating or displacing the boundary layer structures sliding along the riblet and no drag reduction was observed.

Opposition Control

Since selective actuation and hybrid surfaces were unable to alter the flow in a desired manner, we

examined a feedback control scheme to calibrate the strength of actuation. As described in [3], this *v*-opposition control (*VOC*) method senses the normal velocity at a height above a surface and applies a continuous distribution of blowing and suction on the surface of equal and opposite sense to cancel the vertical motion of the fluid. When applied to both walls of a turbulent channel simulation, reductions in drag of as much as 25% were obtained [3]. When applied to only one of the walls of our simulation, a 5% – 10% reduction in drag was obtained.

Since the Formal End to the Grant

Since the grant ended in Dec. 2001, we have continued to make good progress on this, and related, work. To set the work accomplished under this short 1-year grant in better context, I will briefly mention the work accomplished in the subsequent five months.

The capabilities of the *VOC* control scheme were unknown when applied to limited portions of the domain. Therefore, prior to applying this method to discrete devices, we tested *VOC* on continuous strips covering only portions of one wall of the domain. Results indicated reductions of fluctuations near the surface and within the the buffer layer for strips covering as little as 30% of the domain. However, drag reductions were not obtained until considerable dampening was achieved, in this case only when the strip covered more than 80% of the domain.

VOC was next tested on a single, discrete actuator adjacent to its passive “breather” slot. (Some of this work was actually started in December ’01.) The average vertical velocity (\bar{v}) was calculated over an area immediately over the control slot. This \bar{v} value was used to calculate a proper strength of actuation of the driving membrane to produce a counter flow out of the slot. A pair of narrow slots and a pair of wide slots were tested. Unlike previous studies, no jet formation occurred and the actual result was of a local mild heaving of the boundary layer up or down. This motion still provided enough of a disturbance to affect the flow. Figure 4 shows contours of the streamwise velocity near the surface time averaged and span averaged over the centerline of each active slot. The slots appear as regions of high speed flow – caused by the slots acting as shear-free regions, allowing the flow to accelerate over them like flow over a cavity. The active narrow slot shows a distinct low velocity (low shear stress) zone downstream of the actuator measuring approximately 2.5 slot lengths long and a slot width to either side of the centerline (fig. 4, top). A similarly sized region is found aft of the active wide slot, but corresponding instead to an increase in velocity (fig. 4, bottom).

Based on the zone of influence of each *VOC* slot determined in the previous section, a new configuration containing multiple, adjacent, controllable actuators was created for this last part of the study. As seen in figure 5, the slots were uniformly spaced across the span of the domain. All slots share a common sub-surface cavity but each slot has its own subsurface membrane and control region. Two configurations were tested: *Case 1* with 4 actuators (width $L_z = 8h_1$) and *Case 2* with 6 actuators ($L_z = 12h_2$). Results on the drag were compared to a uniform *VOC* covering 10% of the lower surface. As shown in figure 6, the drag for the 10% *VOC* strip was about 10% higher than for the opposing un-actuated surface. In comparison, the drag values for either multiple actuator case are visibly lower than for the 10% strip but still not indicative of a drag reduction. This suggests that discrete actuators may have the same favorable effect as much larger *VOC* strips. In this case, the possible placement of just one or two more rows of actuators might have been enough to yield a drag reduction without the extensive coverage requirement initially indicated by the original *VOC* concept.

Time averaged and span averaged results are shown in figure 7. For both cases, the mean flow starts to accelerate as far as 1.5 slot lengths ahead of the actuators. This was a result of having multiple actuators more closely spaced together which allowed a substantial portion of the near-wall flow to speed up, pulling along upstream fluid. Similar to fig. 4, the narrow slot of *Case 2* (fig.7, top) produces a region of low speed fluid measuring about one slot length long by one slot width wide downstream of the actuators. Likewise, for *Case 1* (fig.7, bottom), a narrow band of higher speed flow surrounded by two bubbles of lower speed flow (low shear stress) develops downstream of the wide slot. These results suggest that there may be a different mechanism for drag reduction here than for a uniform *VOC*

surface. For example, a drag reduction might occur from the combined effect of replacing portions of the plate with several slots behaving like low-shear zones. This suggestion is much like that you and I discussed for a drag-reduction scheme for use in water (Patent pending). Of course, this gain might be negated by areas of high shear stress forming upstream of each hole and increased Reynolds shear stress due to enhanced mixing of fluid at the slots. But if the holes were small and were actively controlled, we might be able to suppress the turbulent mass exchange and reduce the high shear stress footprints to the point of a net drag reduction.

References

- [1] R. Panton, *Self-Sustaining Mechanisms of Wall Turbulence*, Computational Mechanics Publications, 1997, 13-47.
- [2] M. Gad-el-Hak, "Interactive Control of Turbulent Boundary Layers: a Futuristic Overview," *AIAA Journal*, 1994, 32.9:1753-1765.
- [3] H. Choi, P. Moin, and J. Kim, "Active Turbulence Control for Drag Reduction in Wall-Bounded Flows," *J. Fluid Mech.*, 1994, 262:75-110.
- [4] R. Rathnasingham, "System Identification and Active Control of a Turbulent Boundary Layer," FDRL TR 97-6, Fluid Dynamics Research Laboratory, Massachusetts Institute of Technology, 1997.
- [5] A. Crook, A. M. Sadri and N. J. Wood, "The Development and Implementation of Synthetic Jets for the Control of Separated Flow," paper AIAA 99-3176, 1999.
- [6] C. Y. Lee and D. B. Goldstein, "Two-Dimensional Synthetic Jet Simulation," *AIAA Journal*, 40.3:510-516.
- [7] C. Lee and D. B. Goldstein, "DNS of Microjets for Turbulent Boundary Layer Control," AIAA paper 2001-1013, 2001.
- [8] M. J. Walsh, "Viscous drag reduction in boundary layers," *Progress in Astronautics and Aeronautics*, 1990 123:203-259.
- [9] E. Coustols and A. M. Savill, "Turbulent skin-friction drag reduction by active and passive means," *Special Course on Skin-Friction Drag Reduction*, AGARD report 768, 1992, 8:1-55.
- [10] D. B. Goldstein, R. Handler, and L. Sirovich, "Direct numerical simulation of turbulent flow over a modeled riblet covered surface," *J. Fluid Mech.*, 1995, 302:333-376.
- [11] J. Kim, P. Moin, and R. Moser, "Turbulence statistics in fully developed channel flow at low Reynolds number," *J. Fluid Mech.*, 1987, 177: 133-166.

Personnel Supported

Conrad Y. Lee - Graduate Student, The University of Texas at Austin

David B. Goldstein - Associate Professor, The University of Texas at Austin

Publications / Presentations deriving in whole or in part from this project

References [6,7], above

"Simulation of MEMS Suction and Blowing Devices for Turbulent Boundary Layer Control," C. Lee and D. B. Goldstein, AIAA paper 2002-2831, 1st Flow Control Conf., St. Louis, MO, June 2002.

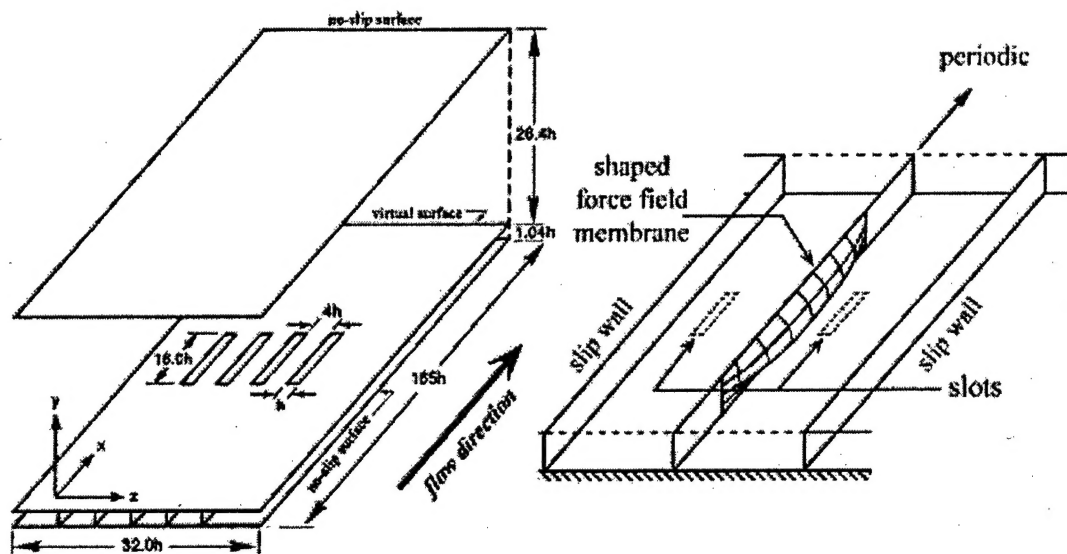


Figure 1: Schematic of channel and actuators and detail of single actuator array

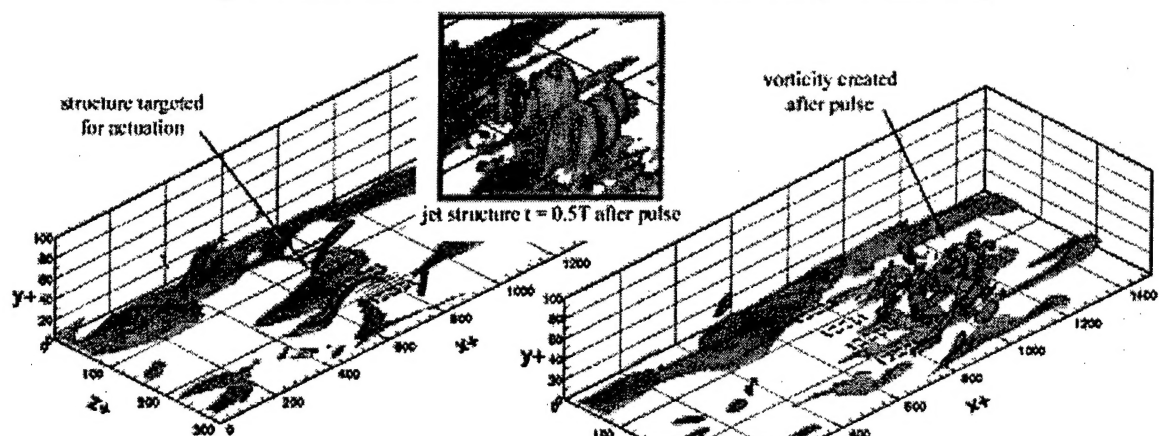


Figure 2(a): Iso-surfaces of enstrophy and Ω_x prior to strong pulse and jet structure detail after pulse

Figure 2(b): Iso-surfaces of enstrophy and Ω_x at $t = 2T$ after strong pulse

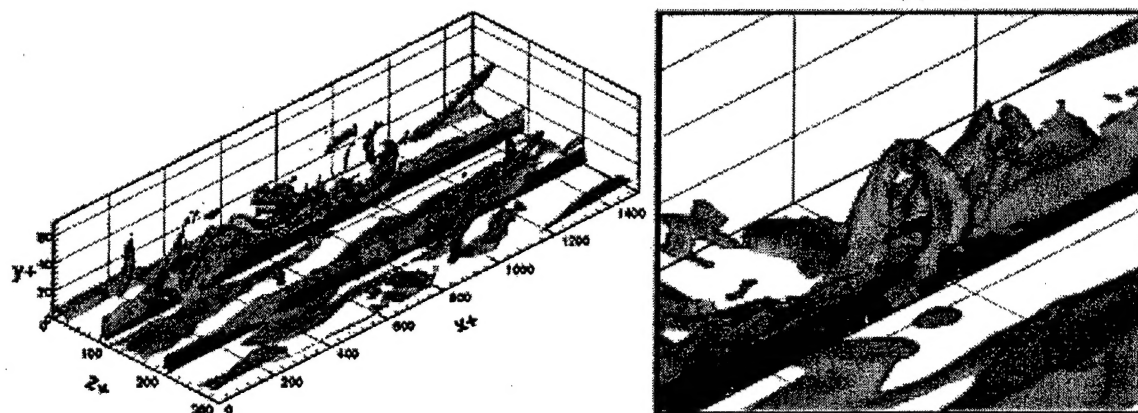


Figure 3(a): Iso-surfaces of enstrophy and Ω_x in channel with two grey riblets and two slots (no control)

Figure 3(b): Iso-surfaces of enstrophy showing jet structure straddling grey riblet ($t = 1.2T$ after pulse)

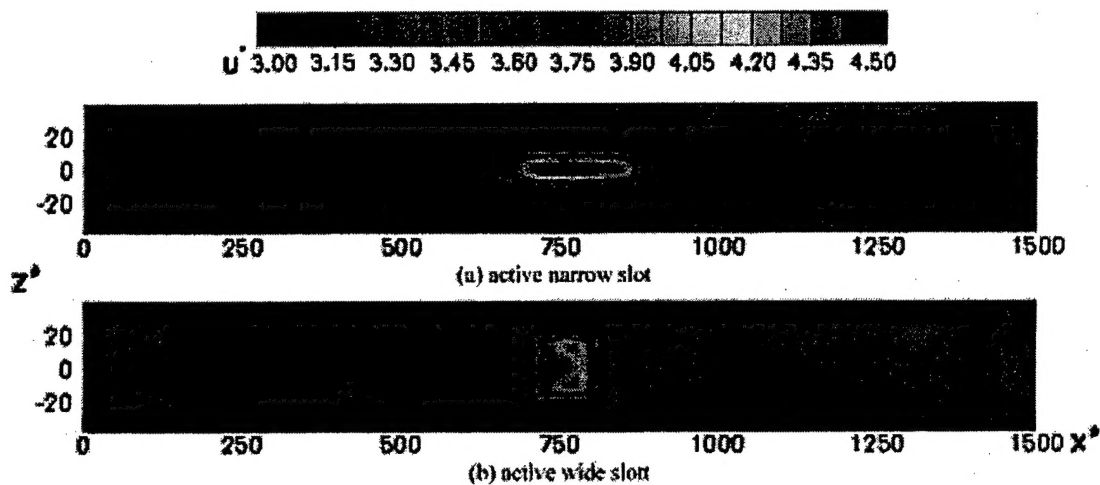


Figure 4: Time averaged contours of streamwise velocity at $y^+ = 3.2$ averaged across centerline of each slot for: (a) active narrow slot and (b) active wide slot

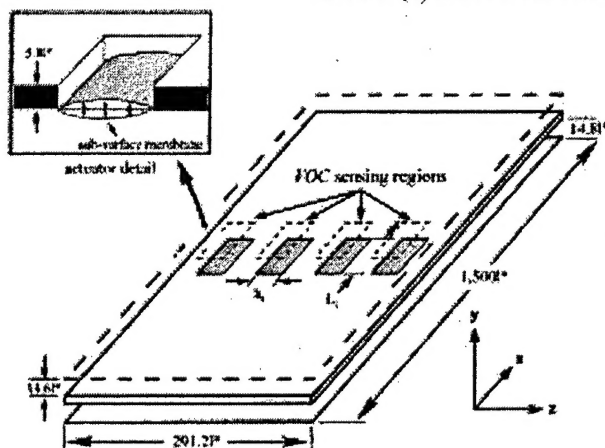


Figure 5: Schematic of multiple actuator geometry with opposition control and actuator detail (Case 1)

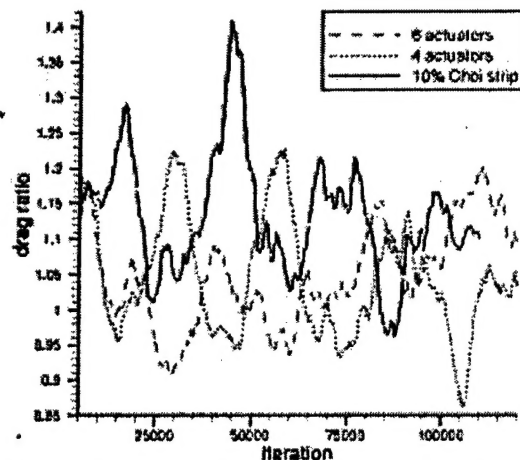


Figure 6: Drag ratios for Case 2 (6 actuators), Case 1 (4 actuators) and 10% VOC strip with respect to the opposing unactuated plate

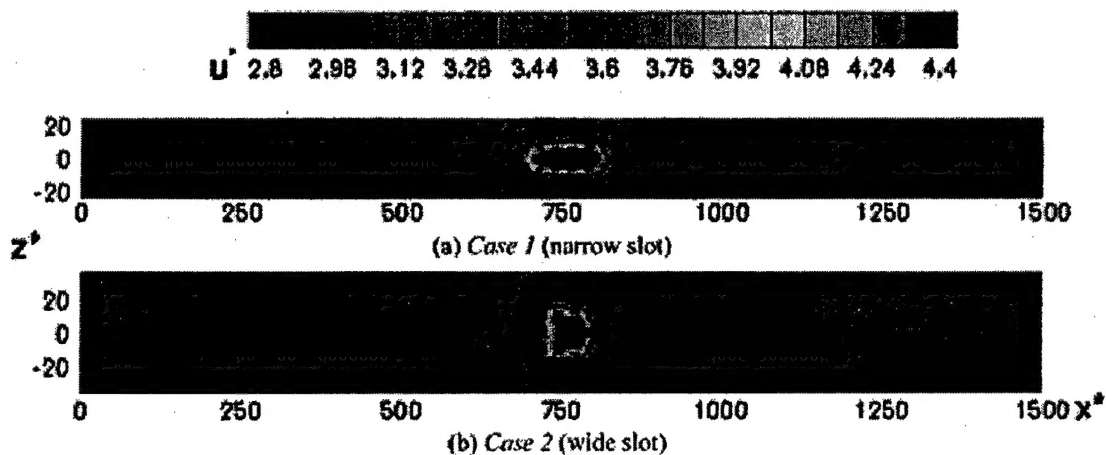


Figure 7: Time averaged contours of streamwise velocity at $y^+ = 3.2$ averaged across centerline of each slot for: (a) Case 1 (narrow slot) and (b) Case 2 (wide slot)